Supporting information

Defect Precise Management Enhances the Efficiency and Electroluminescence Color Stability of Blue Perovskite Light-Emitting Diodes

Chaohui Pi,[a] Jinjiang Wang,*[a] Dandan Li,[a] Zili Chen,[a] Zhixin Dai,[a] Yu Liu,[a] Fan Zhang,[a] Mingchao Xu,[a] Yanhong Deng*[a]

[a] College of Physics and Electronics Engineering, Hengyang Normal University, Hengyang, 421002, China

* Corresponding author: Jinjiang Wang, E-mail: wangjj_391@163.com
Yanhong Deng, E-mail: 2006318dyh@hynu.edu.cn

Experimental sections

Materials

Lead bromide ($PbBr_2$, 99.99%), lead chloride ($PbCl_2$, 99.9%), guanidine hydrobromide (GABr, 99.5%), 1,3,5-tris(1-phenyl-1H-benzimidazol-2-yl)benzene (TPBi, 99.9%), bis(2-(diphenylphosphino)phenyl)ether oxide (DPEPO, 99.5%) and phenethyl ammonium bromide (PEABr, 99.5%) came from Xi'an Yuri Solar Energy Technology Co., LTD. Poly (9-vinyl carbazole) (PVK) (Mv = 25,000 ~ 50,000) was obtained from Acros Organics. Cesium bromide (CsBr, > 99.999%) was purchased from Alfa Aesar. Dimethyl sulfoxide (DMSO, anhydrous, ≥ 99.9%) was supplied from Sigma-Aldrich. All materials were used as received without further purification.

PVK solution preparation

5 mg of PVK was dissolved in 1 mL of chlorobenzene (CB) under continuous stirring until complete dissolution.

Perovskite precursor solution preparation

A quasi-2D perovskite ($PEA_2Cs_{n-1}Pb_nX_{3n+1}$) precursor was prepared by dissolving $PbBr_2$, $PbCl_2$, CsBr, and PEABr in DMSO at a molar ratio of 0.5:0.5:1:0.8. The mixture was stirred for 4 h at room temperature in a N_2-filled glovebox. To obtain precursor solutions with different DPEPO concentrations, 1 mol%, 3 mol%, or 5 mol% of DPEPO (relative to Pb^{2+}) was added to the perovskite precursor solution. Subsequently, 5 mol%, 7.5 mol%, or 10 mol% of GABr (relative to Pb^{2+}) was introduced into the DPEPO-containing solutions to prepare perovskite precursors co-doped with DPEPO and GABr. Prior to perovskite film deposition, all perovskite precursor solutions were filtered through a polytetrafluoroethylene (PTFE-D, 0.45 μm pore size) filter to remove large particle aggregates.

PeLEDs preparation

The ITO substrates (sheet resistance: 10 ~ 15 Ω) were sequentially cleaned in an ultrasonic cleaner using Decon 90, deionized water, ethanol, and isopropanol, followed by drying and ultraviolet-ozone treatment for 15 min before being transferred into a glovebox filled with N_2. The PVK layer was prepared by spin-coating the PVK precursor solution on the ITO at a speed of 5000 rpm for 70 s, annealing at 120℃ for 15 min. After cooling to room temperature, the perovskite precursor solution was spin-coated on the PVK layer at a speed of 4000 rpm for 120 s and then annealed at 75℃ for 5 min to obtain the perovskite films. The as-prepared ITO/PVK/perovskite multilayer structure were transferred into an organic-metal thermal evaporation system for sequential deposition of TPBi (40 nm), LiF (1 nm), and Al (100 nm) under high-vacuum conditions ($< 4 \times 10^{-4}$ Pa). During the deposition process, the growth rates of TPBi (1-2 Å s^{-1}), LiF (0.1 Å s^{-1}), and Al (5 Å s^{-1}) were monitored using quartz crystal oscillator. The devices were encapsulated using UV-curable epoxy and a glass cover after cooling for 20 min. Photoelectronic characterization were subsequently performed under ambient conditions (room temperature, dark environment) to evaluate device performance.

Characterizations

The electrical and optical properties of the devices were simultaneously measured using a computer-controlled Keithley 2400 source meter and a Photo Research PR 655 spectrophotometer, including current density-voltage-luminance (*J-V-L*) curves, electroluminescence (EL) spectra, EL efficiency, current efficiency (CE), power efficiency (PE), and external quantum efficiency (EQE).

The surface morphology of the perovskite films was characterized by scanning electron microscopy (SEM, Gemini Sigma 300). The crystalline structure of the perovskite films was evaluated using X-ray diffraction (XRD, D8 Advance, Bruker). Steady-state photoluminescence (PL) spectra and time-resolved PL (TRPL) decay were measured using a fluorescence spectrometer (Edinburgh FS5). X-ray photoelectron spectroscopy (XPS) was tested with a multifunctional photoelectron spectrometer (Thermo Fisher Scientific, Escalab 250Xi, USA). Absorption spectra were recorded using an ultraviolet-visible spectrophotometer (PerkinElmer, Lambda 365, USA). Fourier-transform infrared spectroscopy (FTIR, IRAffinity-1S, Shimadzu) was employed to probe the chemical interactions between perovskite components and passivators.

Calculation Methods

Density functional theory (DFT) calculations were performed using Material Studio to investigate DPEPO and GUA. The BLYP (Becke-Lee-Yang-Parr) functional is adopted, which belongs to the generalized gradient approximation (GGA) and is suitable for the description of the electronic structure of molecular systems. The double numerical plus polarization (DNP) basis set was selected to balance computational efficiency and accuracy, and is particularly sensitive to molecular polarity and charge distribution. Convergence thresholds were set at 1×10^{-5} Hartree/atom for energy, 2×10^{-3} eV $Å^{-1}$ for atomic forces, and 5×10^{-3} Å for atomic displacement, ensuring reliable results while optimizing computational cost. A gamma-centered k-point mesh of $1 \times 1 \times 1$ was adopted, accounting for system symmetry and dimensionality. Weak Van Der Waals interactions between molecules were explicitly included. Following structural optimization, electrostatic potential analysis and visualization were conducted to interpret molecular properties and support mechanistic understanding.

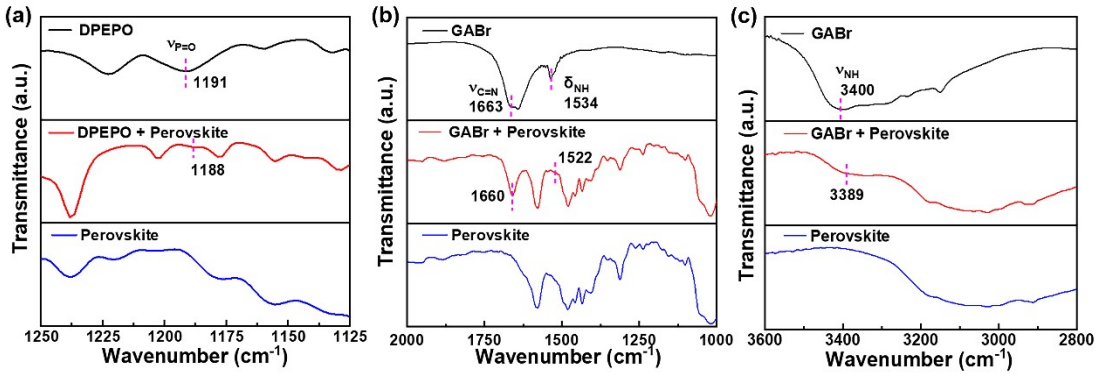

Fig. S1 (a) FTIR spectra of DPEPO, perovskite, and its mixture. (b - c) FTIR spectra of GABr, perovskite, and its mixture.

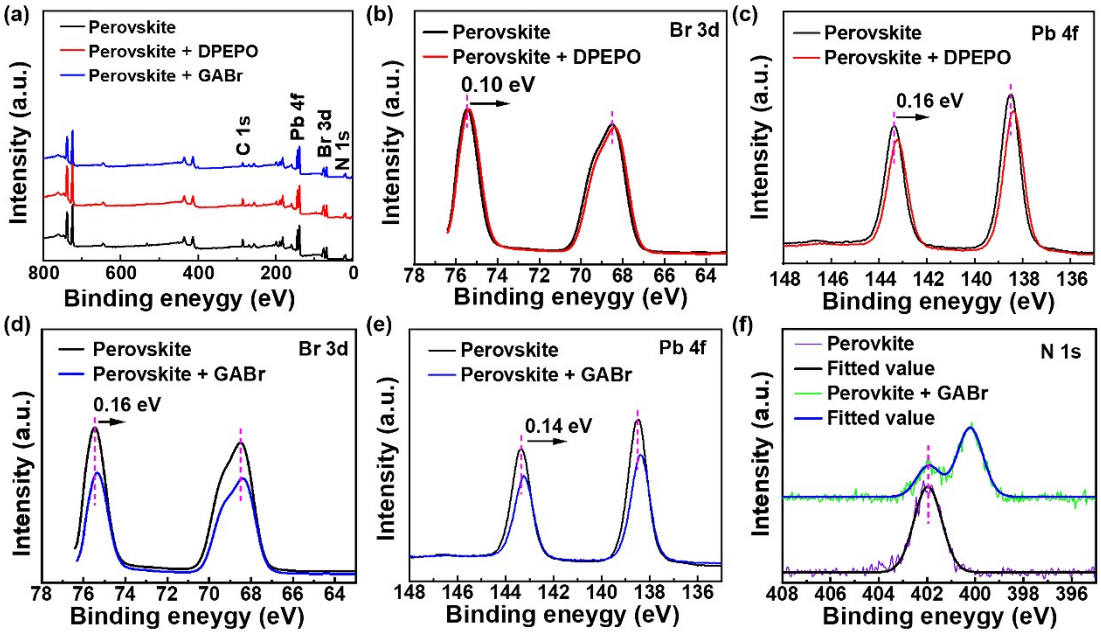

Fig. S2 (a) the full XPS spectra of perovskite, DPEPO-modified perovskite, and GABr-modified perovskite. XPS spectra of (b) Br 3d, (c) Pb 4f of perovskite and DPEPO-modified perovskite. XPS spectra of (d) Br 3d, (e) Pb 4f, and N1s of perovskite and GABr-modified perovskite.

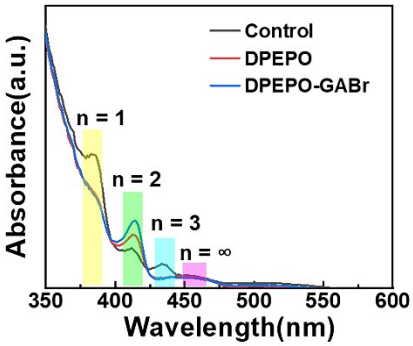

Fig. S3 The UV-Vis absorption spectra of Control, DPEPO-modified and DPEPO-GABr co-modified films

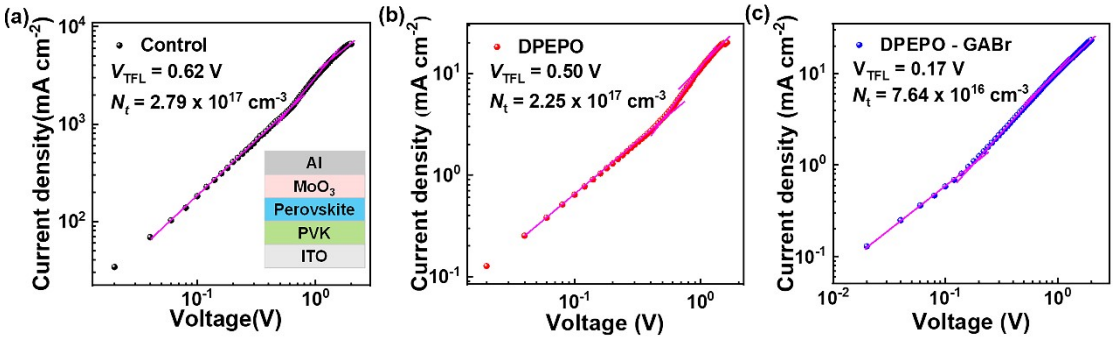

Fig. S4 Current density-voltage curves of different hole-only devices.

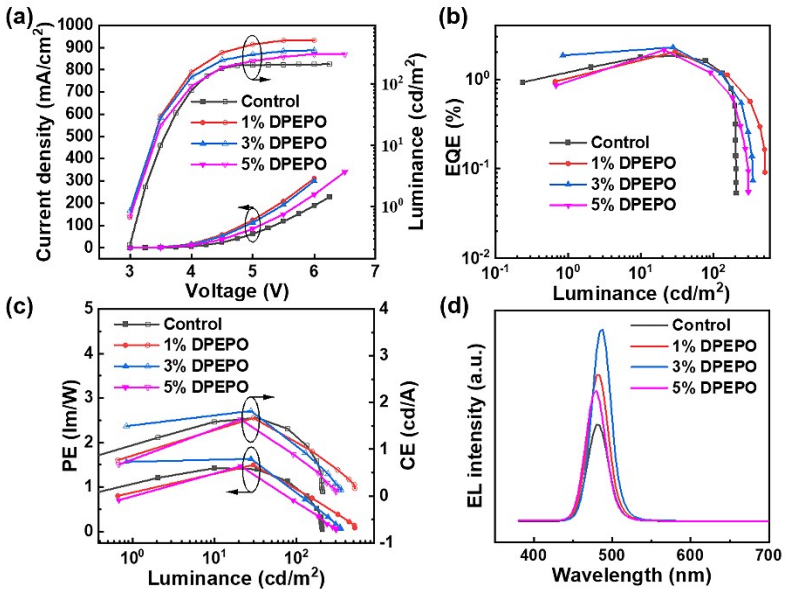

Fig. S5 Photoelectric performance of the PeLEDs with various concentrations DPEPO: (a) Current density-voltage-luminance curves, (b) EQE-luminance curves, (c) PE-luminance curves, (e) EL spectra at the maximum efficiency.

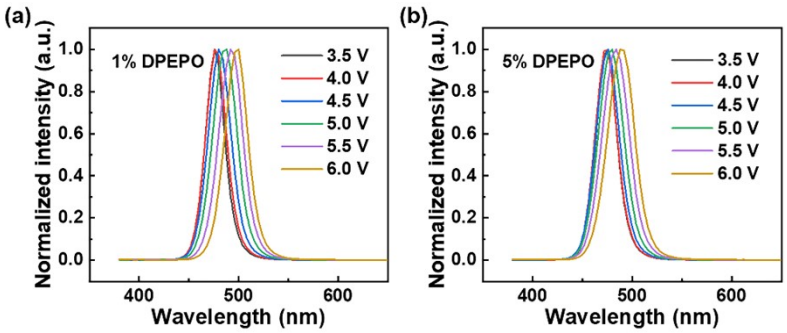

Fig. S6 Normalized EL spectra of the devices with (a) 1% and (b) 5% of DPEPO under different voltages.

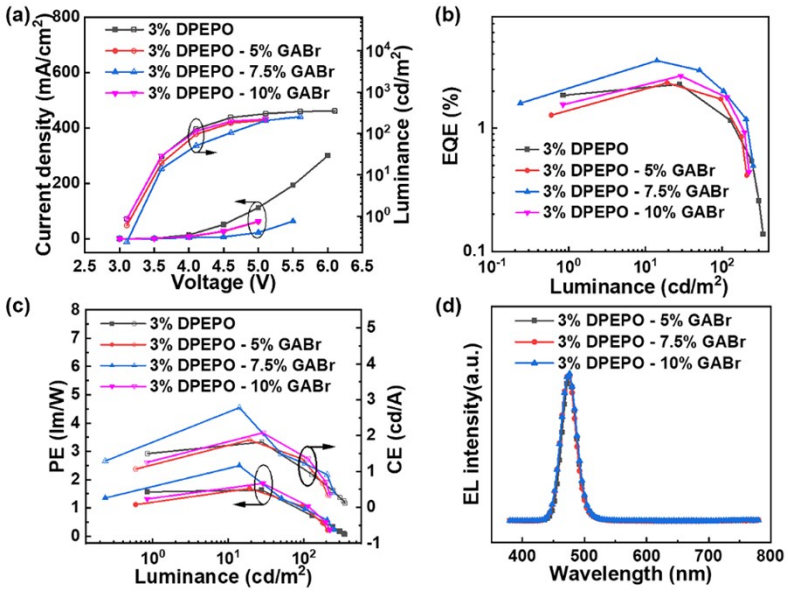

Fig. S7 Photoelectric performance of the PeLEDs with 3% of DPEPO and various concentrations GABr: (a) Current density-voltage-luminance curves, (b) EQE-luminance curves, (c) PE-luminance curves, (e) EL spectra at the maximum efficiency.

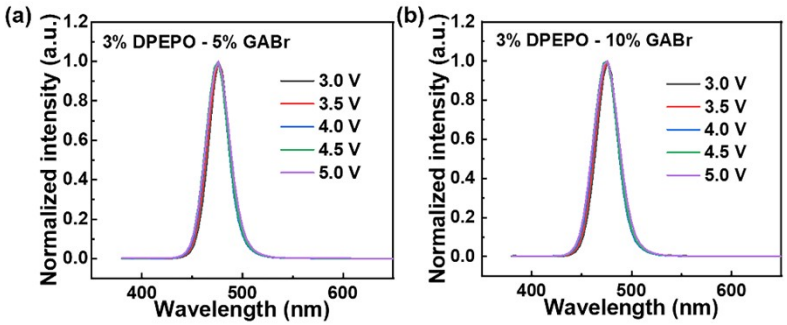

Fig. S8 Normalized EL spectra of the devices with 3% of DPEPO and various concentrations GABr under different voltages.

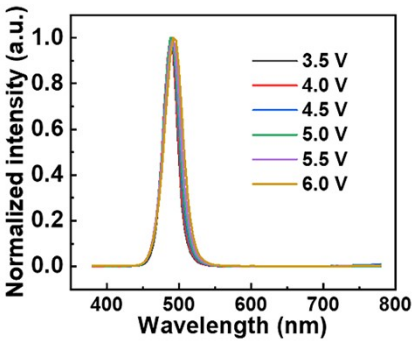

Fig. S9 Normalized EL spectra of the device with KBr under different voltages.

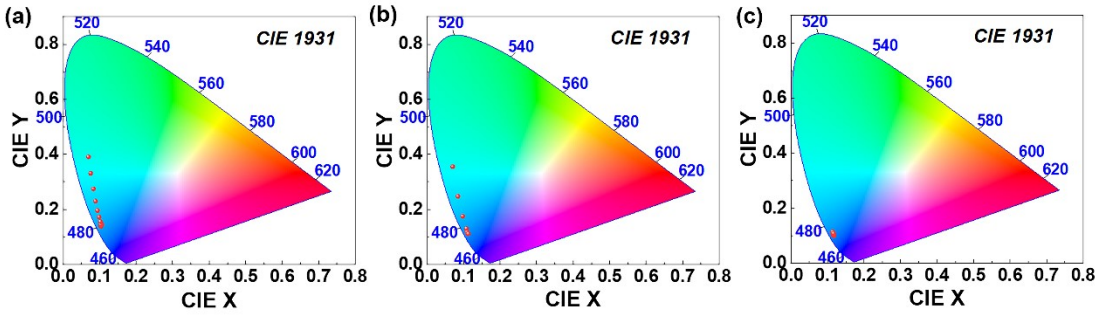

Fig. S10 CIE color coordinates of (a) Control, (b) DPEPO-modified, and (c) DPEPO-GABr co-modified devices under varying voltages.

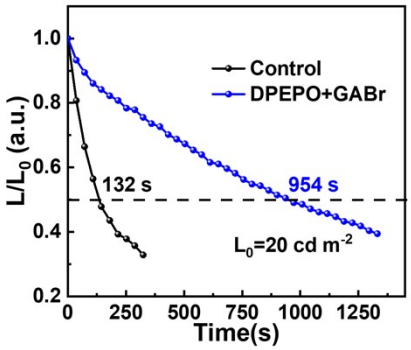

Fig. S11 The operational stability of the Control and DPEPO-GABr co-modified devices.

Table S1 Fitting parameters of the TRPL curves in different perovskite films.

Films	τ_1/ns	A_1/%	τ_2/ns	A_2/%	τ_{ave}/ns
Control	0.92	63.49	4.02	36.51	0.93
DPEPO	1.21	46.78	10.64	53.22	6.24
DPEPO-GABr	1.96	45.52	13.92	54.48	8.48